

Vortex solid-solid phase transition in an untwinned $\text{YBa}_2\text{Cu}_3\text{O}_{7-\delta}$ crystal

D. Giller, A. Shaulov, and Y. Yeshurun

Department of Physics, Institute of Superconductivity, Bar-Ilan University, Ramat-Gan 52900, Israel

J. Giapintzakis*

Department of Physics, University of Illinois at Urbana-Champaign, Urbana, Illinois 61801

(Received 20 January 1999)

Local magnetic measurements vs temperature in an untwinned $\text{YBa}_2\text{Cu}_3\text{O}_{7-\delta}$ crystal reveal an abrupt increase in the local magnetization at a field-dependent temperature, well below the melting line. At the same field and temperature a pronounced kink is observed in the local magnetization vs field curves. The line $B_k(T)$ describing the locations of these anomalies in the field-temperature phase diagram divides the vortex solid phase into two regions characterized by weak and strong pinning. A recently developed model describing the vortex solid-solid disorder-induced phase transition explains quantitatively the observed behavior of $B_k(T)$. From this behavior we infer that the microscopic origin of pinning in $\text{YBa}_2\text{Cu}_3\text{O}_{7-\delta}$ is fluctuations in the charge-carrier mean free path. [S0163-1829(99)00922-4]

The phase diagram of the vortex matter in high-temperature superconductors is a subject of extensive research. Recent experimental¹⁻⁴ and theoretical⁵⁻⁸ works have indicated the existence of at least three vortex phases: a vortex liquid and two distinct vortex solid phases, identified as a quasicrystalline and a highly disordered vortex solids. A vortex solid-liquid phase transition has been demonstrated in $\text{Bi}_2\text{Sr}_2\text{CaCu}_2\text{O}_{8+\delta}$ and $\text{YBa}_2\text{Cu}_3\text{O}_{7-\delta}$ crystals in a variety of experiments, including resistivity, magnetization, and calorimetric measurements.^{3,4,9} A vortex solid-solid phase transition, associated with a sharp onset of a second magnetization peak, has been observed in $\text{Bi}_2\text{Sr}_2\text{CaCu}_2\text{O}_{8+\delta}$ (Ref. 1) and $\text{Nd}_{1.85}\text{Ce}_{0.15}\text{CuO}_{4-\delta}$ crystals.¹⁰ In twinned $\text{YBa}_2\text{Cu}_3\text{O}_{7-\delta}$ the usually observed smeared peak with unresolved onset was difficult to associate with a vortex phase transition. Only recently, measurements in untwinned $\text{YBa}_2\text{Cu}_3\text{O}_{7-\delta}$ revealed a well-resolved second magnetization peak,^{2,11} similar to that observed in $\text{Bi}_2\text{Sr}_2\text{CaCu}_2\text{O}_{8+\delta}$ and $\text{Nd}_{1.85}\text{Ce}_{0.15}\text{CuO}_{4-\delta}$ crystals. However, the peak is still broad and the identification of a specific feature that would possibly mark a phase transition remains unclear.

In this paper we present local magnetic measurements in an untwinned $\text{YBa}_2\text{Cu}_3\text{O}_{7-\delta}$ crystal as a function of temperature, field, and time, revealing anomalies occurring along the *same* line $B_k(T)$ in the field-temperature plane. These include (1) an abrupt increase in the local magnetization vs temperature, (2) a pronounced kink in the magnetization vs field curves, (3) a marked change in the behavior of the magnetic relaxation rate with field, (4) a *time-independent* field B_k , unlike, e.g., the peak field that drifts with time to lower fields. The line $B_k(T)$ divides the vortex solid phase into two regions, characterized by strong and weak pinning at high and low fields, respectively. We identify $B_k(T)$ as a vortex solid-solid phase transition line, equivalent to that found in $\text{Bi}_2\text{Sr}_2\text{CaCu}_2\text{O}_{8+\delta}$ (Ref. 1) and $\text{Nd}_{1.85}\text{Ce}_{0.15}\text{CuO}_{4-\delta}$.¹⁰ It is interesting to note that unlike $\text{Bi}_2\text{Sr}_2\text{CaCu}_2\text{O}_{8+\delta}$ where this line is temperature independent, and $\text{Nd}_{1.85}\text{Ce}_{0.15}\text{CuO}_{4-\delta}$ where it decreases with T , in $\text{YBa}_2\text{Cu}_3\text{O}_{7-\delta}$ B_k is a *nonmonotonic* function of T . We pro-

pose below a universal explanation for the behavior of $B_k(T)$ in all three systems, based on a recent model⁵⁻⁸ describing a disorder-induced phase transition from a quasicrystalline vortex lattice to a highly disordered vortex solid.

The $0.5 \times 0.3 \times 0.02 \text{ mm}^3$ untwinned $\text{YBa}_2\text{Cu}_3\text{O}_{7-\delta}$ crystal ($T_c \approx 93 \text{ K}$) was grown by quenching the tetragonal phase during flux growth.¹² An array of 11 Hall sensors (sensitivity better than 0.1 G), consisting of a GaAs/Al-Ga-As two-dimensional electron-gas layer, was in direct contact with the surface of the crystal. The active area of each sensor was $10 \times 10 \mu\text{m}^2$, separated by $10 \mu\text{m}$.

The local zero-field-cooled magnetization m_{zfc} and the field-cooled magnetization m_{fc} of the $\text{YBa}_2\text{Cu}_3\text{O}_{7-\delta}$ sample were measured as a function of temperature at a constant field, in the range 1–55 kG. In order to compensate for the temperature dependence of the sensors' background, we subtract m_{fc} from m_{zfc} . Figure 1 presents $\Delta m = m_{zfc} - m_{fc}$ for three representative fields: 8, 16, and 40 kG applied parallel

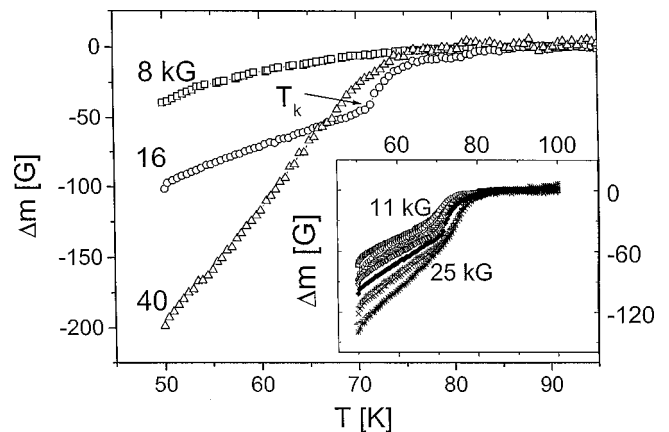


FIG. 1. The difference between the zero-field-cooled and the field-cooled local magnetization in untwinned $\text{YBa}_2\text{Cu}_3\text{O}_{7-\delta}$ plotted vs temperature for 8, 16, and 40 kG fields applied parallel to the c axis. The abrupt increase at $T_k \approx 71 \text{ K}$ for the 16-kG curve is marked by an arrow. The inset shows data for several fields between 11 and 25 kG.

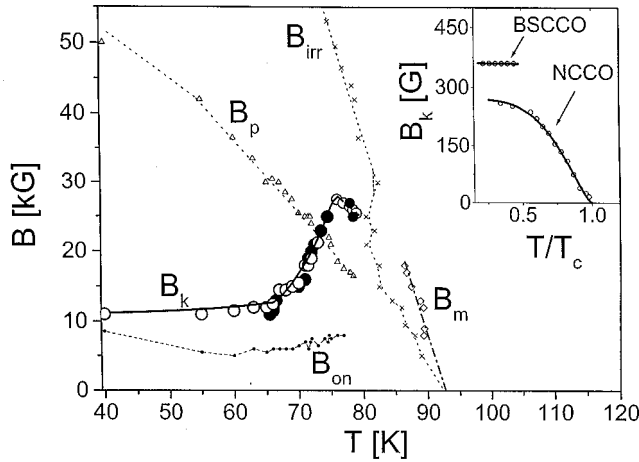


FIG. 2. Magnetic phase diagram for the $\text{YBa}_2\text{Cu}_3\text{O}_{7-\delta}$ crystal showing the temperature T_k of the abrupt increase in $m(T)$ (solid circles), the kink fields B_k in $m(H)$ curves (open circles), the peak field (triangles), the onset field (dots), the irreversibility line (crosses), and the melting line (diamonds). Noisy data in the reversible regime was averaged in order to reveal the jump in the magnetization associated with the melting. This process yielded results consistent with curves obtained in Refs. 4 and 9. No jump could be revealed above 20 kG. Solid line is a theoretical fit. Inset: The vortex solid-solid transition line $B_k(T)$ in $\text{Bi}_2\text{Sr}_2\text{CaCu}_2\text{O}_{8+\delta}$ and $\text{Nd}_{1.85}\text{Ce}_{0.15}\text{CuO}_{4-\delta}$. Solid lines show theoretical fits. Note that in some $\text{Bi}_2\text{Sr}_2\text{CaCu}_2\text{O}_{8+\delta}$ samples, e.g., doped and electron irradiated $\text{Bi}_2\text{Sr}_2\text{CaCu}_2\text{O}_{8+\delta}$ (Ref. 16), B_k increases with temperature.

to the c axis. The 16-kG curve exhibits an abrupt increase at $T_k \approx 71$ K, as indicated in the figure. A similar feature is observed for all fields between 11 and 25 kG, see inset to Fig. 1. The temperature T_k increases with the field, as described in Fig. 2 (solid circles). This feature disappears below 11 kG and above 25 kG where a smooth curve is observed, as represented in Fig. 1 by the 8- and 40-kG curves, respectively. Note, however, the change in the shape of these two curves. While the 40-kG curve exhibits a linear increase over a wide temperature range, the 8-kG curve is nonlinear.

The local magnetization of the same sample was measured as a function of field at a constant temperature, in the range 40–90 K. Typical results, for $T = 60$ K, are shown in Fig. 3. A well-resolved second peak, similar to that reported for $\text{Bi}_2\text{Sr}_2\text{CaCu}_2\text{O}_{8+\delta}$ (Ref. 1) and $\text{Nd}_{1.85}\text{Ce}_{0.15}\text{CuO}_{4-\delta}$ ¹⁰ is observed here. We call attention to the pronounced kink at a field B_k in between the onset field B_{on} and the peak field B_p as indicated in Fig. 3. The temperature dependence of B_k is shown by open circles in the magnetic phase diagram of Fig. 2, together with the irreversibility line (crosses—determined from the coincidence of the ascending and descending branches of the magnetization curves) and the melting line [diamonds—determined by a discontinuity in $\Delta m(T)$ in the reversible regime]. A central result of this work is that the line defined by B_k (open circles) coincides with the line defined by T_k (solid circles), suggesting a phase transition in the vortex system across this line. Evidently, the line defined by $B_k(T)$ divides the irreversible phase into two regions, suggesting that B_k is a transition line between two solid phases of the vortex system.

Also shown in Fig. 3 is the evolution of the second peak with time in the time range 10–3000 sec (solid squares) and

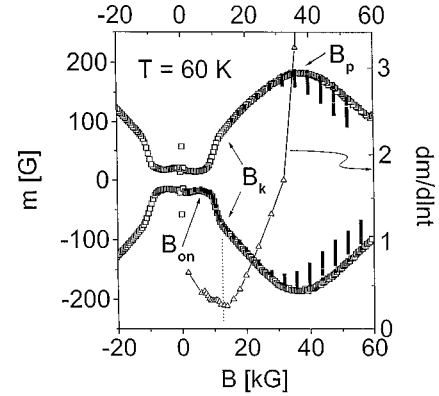


FIG. 3. Local magnetization of the $\text{YBa}_2\text{Cu}_3\text{O}_{7-\delta}$ sample as a function of field as measured at $T = 60$ K. The solid squares describe the evolution of $m(B)$ with time between 10 and 3000 sec. The relaxation rate (right-hand ordinate) is indicated by triangles.

the relaxation rate $dm/d \ln t$ vs field (triangles). Both the onset field and the peak field drift with time (to higher and lower fields, respectively), whereas the kink field B_k is time independent. As indicated in the figure, the relaxation rate $dm/d \ln t$ (triangles) exhibits a minimum at B_k , a behavior consistent with the observation of time independent B_k .

The temperature dependence of the peak field B_p , in the short-time limit, is also included in Fig. 2 (triangles). As mentioned above, the peak field drifts with time to lower fields, indicating that $B_p(T)$ cannot be a phase-transition line; it probably signifies a crossover in the dynamics, from elastic to plastic flux creep, as discussed by Abulafia *et al.*¹³ Note that the temperature dependence of B_p is qualitatively different from that of the phase-transition line B_k . The lines $B_k(T)$ and $B_p(T)$ meet at approximately 73 K above which the anomalous second peak splits into two peaks, as previously reported by Deligiannis *et al.*¹¹ A kink in the magnetization curve is now observed in between the two peaks. The B_p and the B_k data of Fig. 2, above the crossing point $T = 73$ K, represent the location of the lower peak and the kink that appears above it, respectively.

The $B_k(T)$ curve of $\text{YBa}_2\text{Cu}_3\text{O}_{7-\delta}$, Fig. 2, is markedly different from the corresponding curves obtained, from magnetization curves, in $\text{Bi}_2\text{Sr}_2\text{CaCu}_2\text{O}_{8+\delta}$ (Ref. 1) and $\text{Nd}_{1.85}\text{Ce}_{0.15}\text{CuO}_{4-\delta}$ (Ref. 10) crystals, see inset to Fig. 2. While $B_k(T)$ is approximately constant in $\text{Bi}_2\text{Sr}_2\text{CaCu}_2\text{O}_{8+\delta}$ and decreases monotonically with temperature in $\text{Nd}_{1.85}\text{Ce}_{0.15}\text{CuO}_{4-\delta}$, it is a nonmonotonic function of temperature in the untwinned $\text{YBa}_2\text{Cu}_3\text{O}_{7-\delta}$. These pronounced differences can be explained quantitatively within the framework of a recent theory^{5–8} describing a mechanism for a disorder-induced phase transition, from a relatively ordered vortex lattice, to a highly disordered vortex solid. The essence of this theory is that the vortex phase diagram is determined by the interplay between three energy scales: the vortex elastic energy E_{el} , the energy of thermal fluctuations E_{th} , and the pinning energy E_{pin} . At low temperatures, where E_{th} is relatively small, the vortex solid-solid phase-transition line $B_k(T)$ is the crossing line between $E_{\text{el}}(B, T)$ and $E_{\text{pin}}(B, T)$ surfaces. Both energies depend on the superconductor parameters—the penetration depth λ , the correlation length ξ , the pinning parameter γ , and the anisotropy

ratio ε . In $\text{Bi}_2\text{Sr}_2\text{CaCu}_2\text{O}_{8+\delta}$, B_k persists up to only 40 K, well below T_c . In this temperature range ($T \ll T_c$) all the superconductor parameters are almost temperature independent. As a result, the line defined by $E_{\text{el}} = E_{\text{pin}}$ is approximately temperature independent. In $\text{Nd}_{1.85}\text{Ce}_{0.15}\text{CuO}_{4-\delta}$ ($T_c \approx 23$ K) and $\text{YBa}_2\text{Cu}_3\text{O}_{7-\delta}$ ($T_c \approx 93$ K) B_k persists up to at least $T/T_c = 0.93$ and 0.86 , respectively, and therefore the temperature dependence of the superconductor parameters affect $E_{\text{pin}}(T)$ and $E_{\text{el}}(T)$, and consequently $B_k(T)$. As discussed below, $B_k(T)$ depends strongly on the specific microscopic pinning mechanism—different mechanisms may cause either an increase or a decrease of B_k with temperature. As a matter of fact, the specific behavior of $B_k(T)$ may serve as a probe for the microscopic pinning mechanism. Thus, the decrease of $B_k(T)$ in $\text{Nd}_{1.85}\text{Ce}_{0.15}\text{CuO}_{4-\delta}$ up to the close vicinity of T_c , and the weak increase of B_k up to 66 K in $\text{YBa}_2\text{Cu}_3\text{O}_{7-\delta}$, both find a natural explanation as a disorder-induced phase transition, taking into account different origins for the pinning mechanism in these particular samples. Quantitative fits of the experimental data for the three samples show good agreement with the theoretical predictions. A detailed explanation of the fit procedure is outlined in the next paragraphs.

Near the transition, for temperatures below the depinning temperature T_{dp} (defined below), $E_{\text{el}} = \varepsilon \varepsilon_0 c_L^2 a_0$ and $E_{\text{pin}} = U_{\text{dp}}(L_0/L_c^0)^{1/5}$, where $\varepsilon_0 = (\Phi_0/4\pi\lambda)^2$ is the vortex line tension, $c_L = 0.1-0.3$ is the Lindenmann number, $U_{\text{dp}} = (\gamma \varepsilon^2 \varepsilon_0 \xi^4)^{1/3}$ is the single vortex depinning energy, $L_0 \approx 2\varepsilon a_0$ is the characteristic length for the longitudinal fluctuations, $L_c^0 = (\varepsilon^4 \varepsilon_0^2 \xi^2 / \gamma)^{1/3}$ is the size of the coherently pinned segment of the vortex, and γ is the disorder parameter. The equation $E_{\text{el}} = E_{\text{pin}}$ then yields $B_k = B_0 [U_0/U_{\text{dp}}]^3$, where $B_0 = c_L^2 \Phi_0 / \xi^2$ and $U_0 = c_L \varepsilon \varepsilon_0 \xi / 2^{11/6}$. Thus, the temperature dependence of B_k has its origin in the temperature dependence of ξ , λ , and γ . While the temperature dependence of ξ and λ is universal, that of γ depends on the pinning mechanism. Pinning may be caused by spatial fluctuations of T_c (“ δT_c pinning”) or of the charge-carrier mean free path l (“ δl pinning”) near a lattice defect. Spatial variations of T_c lead to a spatial modulation of the linear and quadratic terms in the Ginzburg-Landau (GL) free-energy functional, whereas variations of the mean free path affect the gradient of the order parameter in the GL functional (for further discussion, see Ref. 14, p. 1141). Our fitting procedure demonstrates that the temperature dependence of $B_k(T)$ determines unequivocally which one of these two pinning mechanisms dominates, as these two pinning mechanisms give rise to qualitatively different behavior of $B_k(T)$: For δT_c pinning $\gamma \propto 1/\lambda^4$ and

$$B_k(T) = B_k(0) [\xi(T)/\xi(0)]^{-3} = B_k(0) [1 - (T/T_c)^4]^{3/2}, \quad (1)$$

i.e., B_k decreases monotonically with T , whereas for δl pinning $\gamma \propto 1/(\lambda \xi)^4$, and

$$B_k(T) = B_k(0) \xi(T)/\xi(0) = B_k(0) [1 - (T/T_c)^4]^{-1/2}, \quad (2)$$

i.e., B_k increases with T . The solid line in the inset to Fig. 2 shows a one-parameter fit of Eq. (1) to the B_k data for $\text{Nd}_{1.85}\text{Ce}_{0.15}\text{CuO}_{4-\delta}$ yielding $B_k(0) = 270$ G. The increase of B_k with temperature observed in $\text{YBa}_2\text{Cu}_3\text{O}_{7-\delta}$ indicates a

δl -pinning mechanism, supporting the conclusions of Griesen *et al.*¹⁵ A one-parameter fit of Eq. (2) fits well the B_k data for $\text{YBa}_2\text{Cu}_3\text{O}_{7-\delta}$ up to $T = 66$ K, as shown by the solid line in Fig. 2, yielding $B_k(0) = 11$ kG. Above 66 K, $B_k(T)$ exhibits a dramatic increase, which may be attributed to a strong decrease of the pinning energy E_{pin} , suggesting that for our $\text{YBa}_2\text{Cu}_3\text{O}_{7-\delta}$ the depinning temperature $T_{\text{dp}} = 66$ K. (At T_{dp} , the amplitude of the vortex line thermal fluctuations becomes comparable to ξ and, as a result, the effective disorder is dramatically weakened.) This value of T_{dp} will be further justified below. To fit the data above T_{dp} we note that at 66 K, at the solid-solid transition field, $E_{\text{el}} = E_{\text{pin}} \approx 80$ K, both comparable to kT , and thus one must take into account the contribution of the thermal energy. This may be accomplished by introducing the strong thermal smearing of the pinning disorder through an exponential increase of the Larkin length, $L_c = (T_{\text{dp}}/T) L_c^0 \exp\{c[(T/T_{\text{dp}})^3 - 1]\}$ for $T > T_{\text{dp}}$, where c is a number of order 1.^{7,14} Introducing this expression of L_c in $E_{\text{pin}} = U_{\text{dp}}(L_0/L_c)^{1/5}$, and equating E_{pin} to E_{el} , yields the solid line in Fig. 2 between 66 and 75 K, using the *same* parameters as above, i.e., $T_{\text{dp}} = 66$ K and $B_k(0) = 11$ kG. This approach is valid only in the vicinity of T_{dp} . Our calculations show that above 75 K, $L_c > L_0$ and the pinning energy is now given by $E_{\text{pin}} \equiv \sqrt{\gamma \xi^2 L_0}$,⁶ i.e., no longer dependent on L_c . Therefore, the fast decrease of E_{pin} with temperature is moderated, and the increase of the superconducting parameters with temperature causes B_k to decrease.

For $\text{Bi}_2\text{Sr}_2\text{CaCu}_2\text{O}_{8+\delta}$ (inset to Fig. 2), B_k is found only at relatively low temperatures, over a small range of T/T_c , and therefore it shows no temperature dependence. In this particular case, the data may be fitted with either Eq. (1) or Eq. (2) with one parameter, $B_k(0) = 360$ G. We note that in some samples, e.g., doped and electron irradiated $\text{Bi}_2\text{Sr}_2\text{CaCu}_2\text{O}_{8+\delta}$,¹⁶ B_k increases with temperature, suggesting a δl -pinning mechanism in these samples.

As it is clear from Figs. 1 and 2, the local magnetization vs temperature exhibits an abrupt increase only in a limited field range, corresponding to the increasing branch of $B_k(T)$. Crossing this branch by raising temperature at a constant field corresponds to a phase transition from a disordered vortex state with a relatively high persistent current to a quasi-ordered state with low current. This phase transition is accompanied by a burst of flux lines penetrating the sample, manifested by an abrupt increase in the magnetization. This feature is absent in further raising the temperature to cross the $B_k(T)$ line along its decreasing branch. This is because the system transforms from a quasiordered to an highly disordered state, i.e., flux should be expelled from the sample, a process that is impeded by the presence of an external field. The transition in this case is manifested by a slight decrease in dm/dT indicated by small solid circles in the descending part of $B_k(T)$; see Fig. 2. For fields larger than 25 kG and smaller than 11 kG, raising temperature does not lead to crossing of the $B_k(T)$ line and thus no sign of a phase transition is observed in $m(T)$ measurements. Similar arguments explain our observation of a change in dm/dT in $\text{Nd}_{1.85}\text{Ce}_{0.15}\text{CuO}_{4-\delta}$ on crossing its B_k line,¹⁷ and the absence of such anomalies in the $m(T)$ curves of $\text{Bi}_2\text{Sr}_2\text{CaCu}_2\text{O}_{8+\delta}$.

As we have mentioned, the three fields indicated in Fig. 3, B_{on} , B_k , and B_p , characterize the anomalous second peak in the untwinned $\text{YBa}_2\text{Cu}_3\text{O}_{7-\delta}$. We identified B_k as a transition field between two vortex solid phases,¹⁰ and B_p as related to a dynamic crossover from elastic (collective) to plastic flux creep. The onset field B_{on} may be interpreted as signifying a dynamic crossover between two different collective creep regimes. For example, a crossover from a single vortex regime below B_{on} (where the pinning energy U does not depend on field) to a small bundle regime above B_{on} (where U increases sharply with field) can lead to a sharp increase in the magnetization.^{14,18} Similarly, a crossover from small to large bundles,¹⁴ which may occur at high temperatures, would give rise to an increase in the magnetization in the quasiordered state. Thus, we conclude that different mechanisms govern the shape of the second peak: At low fields, around B_{on} , $m(H)$ is determined by a crossover within collective states; a solid-solid phase transition shapes the $m(H)$ curve at B_k ; at high fields, around B_p , $m(H)$ is determined by a crossover from collective to plastic creep. The splitting of the second magnetization peak at high temperatures may be related to the complex dynamic behavior observed in our sample and requires more investigations.

In summary, local magnetic measurements in an untwinned $\text{YBa}_2\text{Cu}_3\text{O}_{7-\delta}$ crystal as a function of temperature, field, and time, exhibit anomalies along the *same* line $B_k(T)$, identified as a transition between two vortex solid phases, similar to that reported for $\text{Bi}_2\text{Sr}_2\text{CaCu}_2\text{O}_{8+\delta}$ and $\text{Nd}_{1.85}\text{Ce}_{0.15}\text{CuO}_{4-\delta}$. The temperature dependence of the phase-transition lines in these three systems, though markedly different, can be quantitatively explained on the basis of

the same model describing a disorder-induced phase transition, from a quasiordered to an highly disordered vortex solid phase.

The vortex phase diagram obtained in this work for untwinned $\text{YBa}_2\text{Cu}_3\text{O}_{7-\delta}$ supports the validity of the phase diagram recently published by Nishizaki, Naito, and Kobayashi.² The novel results of the present work can be summarized as follows: (a) The observation of a pronounced feature—a sharp kink in the magnetization curves—that signifies the disorder-driven phase transition. (b) Field, temperature, and time-dependent measurements reveal anomalies occurring along the same line $B_k(T)$. (c) The $B_k(T)$ data can be *quantitatively* fitted to a model describing a disorder-induced transition from a quasiordered to a highly disordered vortex solid phase. (d) The same model can explain the markedly different behavior of the transition line obtained in three different systems, namely, $\text{YBa}_2\text{Cu}_3\text{O}_{7-\delta}$, $\text{Nd}_{1.85}\text{Ce}_{0.15}\text{CuO}_{4-\delta}$ and $\text{Bi}_2\text{Sr}_2\text{CaCu}_2\text{O}_{8+\delta}$. (e) The qualitative behavior of $B_k(T)$ determines unequivocally the microscopic origin of the pinning mechanism, distinguishing between pinning arising from spatial fluctuations of T_c or of the charge-carriers mean free path.

We acknowledge discussions with E. Zeldov and R. Prozorov. We thank H. Shtrikman and Y. Abulafia for growing the GaAs heterostructures. This work was partially supported by The Israel Science Foundations and by the Heinrich Hertz Minerva Center for High Temperature Superconductivity. Y.Y. and A.S. acknowledge support from the German Israeli Foundation (G.I.F.). D.G. acknowledges support from the Clore Foundation.

*Present address: Foundation for Research and Technology—Hellas, Institute of Electronic Structure and Laser, 711 10 Heraklion, Greece.

¹B. Khaykovich, E. Zeldov, D. Majer, T. W. Li, P. H. Kes, and M. Konczykowski, *Phys. Rev. Lett.* **76**, 2555 (1996).

²T. Nishizaki, T. Naito, and N. Kobayashi, *Phys. Rev. B* **58**, 11 169 (1998).

³E. Zeldov, D. Majer, M. Konczykowski, V. B. Geshkenbein, V. M. Vinokur, and H. Shtrikman, *Nature (London)* **375**, 373 (1995).

⁴A. Schilling, R. A. Fisher, N. E. Phillips, U. Welp, W. K. Kwok, and G. W. Crabtree, *Phys. Rev. Lett.* **78**, 4833 (1997).

⁵T. Giamarchi and P. L. Doussal, *Phys. Rev. Lett.* **72**, 1530 (1994); *Phys. Rev. B* **55**, 6577 (1997).

⁶V. Vinokur, B. Khaykovich, E. Zeldov, M. Konczykowski, R. A. Doyle, and P. Kes, *Physica C* **295**, 209 (1998).

⁷D. Ertas and D. R. Nelson, *Physica C* **272**, 79 (1996).

⁸J. Kierfeld, *Physica C* **300**, 171 (1998).

⁹H. Safar, P. L. Gammel, D. A. Huse, D. J. Bishop, W. C. Lee, J. Giapintzakis, and D. M. Ginsberg, *Phys. Rev. Lett.* **70**, 3800 (1993); H. Safar, P. L. Gammel, D. A. Huse, G. B. Alers, D. J. Bishop, W. C. Lee, J. Giapintzakis, and D. M. Ginsberg, *Phys. Rev. B* **52**, 6211 (1995); M. Willemin, A. Schilling, H. Keller, C. Rossel, J. Hofer, U. Welp, W. K. Kwok, R. J. Olsson, and G. W. Crabtree, *Phys. Rev. Lett.* **81**, 4236 (1998).

¹⁰D. Giller, A. Shaulov, R. Prozorov, Y. Abulafia, Y. Wolfus, L.

Burlachkov, Y. Yeshurun, E. Zeldov, V. M. Vinokur, J. L. Peng, and R. L. Greene, *Phys. Rev. Lett.* **79**, 2542 (1997). Note that in this reference B_{on} is actually the kink field and not the onset field.

¹¹K. Deligiannis, P. A. L. de Groot, S. Pinfold, R. Langan, R. Gagnon, and L. Taillefer, *Phys. Rev. Lett.* **79**, 2121 (1997).

¹²J. P. Rice and D. M. Ginsberg, *J. Cryst. Growth* **109**, 432 (1991).

¹³Y. Abulafia, A. Shaulov, Y. Wolfus, R. Prozorov, L. Burlachkov, Y. Yeshurun, D. Majer, E. Zeldov, H. Wühl, V. B. Geshkenbein, and V. M. Vinokur, *Phys. Rev. Lett.* **77**, 1596 (1996).

¹⁴G. Blatter, M. V. Feigelman, V. B. Geshkenbein, A. I. Larkin, and V. M. Vinokur, *Rev. Mod. Phys.* **66**, 1125 (1994).

¹⁵R. Griessen, Wen Hai-hu, A. J. J. van Dalen, B. Dam, J. Rector, H. G. Schnack, S. Libbrecht, E. Osquiguil, and Y. Bruynseraede, *Phys. Rev. Lett.* **72**, 1910 (1994); A. J. J. van Dalen, R. Griessen, S. Libbrecht, Y. Bruynseraede, and E. Osquiguil, *Phys. Rev. B* **54**, 1366 (1996).

¹⁶M. F. Goffman, J. A. Herbsommer, F. de la Cruz, T. W. Li, and P. H. Kes, *Phys. Rev. B* **57**, 3663 (1998); D. T. Fuchs, E. Zeldov, T. Tamegai, S. Ooi, M. Rappaport, and H. Shtrikman, *Phys. Rev. B* **80**, 4971 (1998); B. Khaykovich, M. Konczykowski, E. Zeldov, R. A. Doyle, D. Majer, P. H. Kes, and T. W. Li, *Phys. Rev. B* **56**, R517 (1997).

¹⁷D. Giller, A. Shaulov, and Y. Yeshurun (unpublished).

¹⁸L. Krusin-Elbaum, L. Civale, V. M. Vinokur, and F. Holtzberg, *Phys. Rev. Lett.* **69**, 2280 (1992).